(28) Varanarajan, K.; Boyer, R. F. *Polymer* **1982**, *23*, 314.
(29) Johari, G. P. *Polymer* **1986**, *27*, 866.
(30) Johari, G. P.; Monnerie, L. *J. Polym. Sci., Poly. Phys. Ed.* **1986**, *24*, 2049.
(31) Cochrane, J.; Harrison, G.; Lamb, J.; Phillips, D. W. *Polymer* **1980**, *21*, 837.
(32) Plazek, D. J.; Ngai, K. L.; Rendell, R. W. *Polym. Eng. Sci.* **1984**, *24*, 1111.
(33) Ngai, K. L.; Plazek, D. J. *J. Polym. Sci., Polym. Phys. Ed.* **1986**, *24*, 619.
(34) Ngai, K. L.; Plazek, D. J.; Deo, S. S. *Macromolecules* **1987**, *20*, 3047.
(35) McKinney, J. E.; Belcher, H. V. *J. Res. Natl. Bur. Stand., Sect. A* **1963**, *67A*, 43.
(36) Plazek, D. J.; O'Rourke, V. M. *J. Polym. Sci., Polym. Phys. Ed.* **1971**, *9*, 209.
(37) Williams, M. L.; Ferry, J. D. *J. Colloid Sci.* **1954**, *9*, 479.
(38) Kovacs, A. J. *Adv. Polym. Sci.* **1963**, *3*, 394.
(39) Kovacs, A. J.; Stratton, R. A.; Ferry, J. D. *J. Phys. Chem.* **1963**, *67*, 152.
(40) Plazek, D. J. *Polym. J. (Tokyo)* **1980**, *12*, 43.
(41) Plazek, D. J. *J. Polym. Sci., Polym. Phys. Ed.* **1982**, *20*, 729.
(42) Rendell, R. W.; Aklonis, J. J.; Ngai, K. L.; Fong, G. R. *Macromolecules* **1987**, *20*, 1070.
(43) Mead, D. J.; Fuoss, R. M. *J. Am. Chem. Soc.* **1941**, *63*, 2832.
(44) Ishida, Y.; Matsuo, M.; Yamafuji, K. *Kolloid Z. Z. Polym.* **1961**, *180*, 108.
(45) Saito, S.; Nakajima, T. *J. Appl. Polym. Sci.* **1959**, *11*, 93.
(46) Sasabe, H.; Moynihan, C. T. *J. Polym. Sci., Polym. Phys. Ed.* **1978**, *16*, 1447.
(47) Nozaki, R.; Mashimo, S. *J. Chem. Phys.* **1986**, *84*, 3575.
(48) Mashimo, S.; Nozaki, R.; Yagihara, S.; Takeishi, S. *J. Chem. Phys.* **1982**, *77*, 6259.
(49) Rendell, R. W.; Ngai, K. L.; Mashimo, S. *J. Chem. Phys.* **1987**, *87*, 2359.
(50) Williams, G.; Watts, D. C. In *NMR Basic Principles and Progress*; Diehl, P., Fluck, E., Kosfeld, R., Eds.; Springer-Verlag: Berlin, 1971; Vol. 4, p 271.
(51) Williams, G. *Trans. Faraday Soc.* **1964**, *60*, 1548.
(52) Ferry, J. D.; Landel, R. F. *Kolloid-Z.* **1956**, *148*, 1. Williams, M. L.; Ferry, J. D. *J. Colloid Sci.* **1955**, *10*, 474. Fujino, K.; Senshu, K.; Kawai, H. *J. Colloid Sci.* **1961**, *16*, 1.
(53) Fytas, G.; Wang, C. H.; Fischer, E. W.; Mehler, K. *J. Polym. Sci., Polym. Phys. Ed.* **1986**, *24*, 1859.
(54) See collection of papers: Oppenheim, I.; Schuler, IK. E.; Weiss, G. H. *Stochastic Process in Chemical Physics*; Massachusetts Institute of Technology: Cambridge, MA, 1977.
(55) Berne, B.; Pecora, B. *Dynamic Light Scattering*; Wiley: New York, NY, 1980.
(56) Chu, B. *Polym. J. (Tokyo)* **1985**, *17*, 225. Chu, B. *Laser Light Scattering*; Academic: New York, NY, 1974.
(57) Helfand, E. *Science (Washington, D.C.)* **1984**, *226*, 647.
(58) See: Sudarshan, E. C. G.; Mukunda, N. *Classical Mechanics: A Modern Perspective*; Wiley: New York, NY, 1974.
(59) Ngai, K. L. *Comments Solid State Phys.* **1979**, *9*, 121.
(60) Rajagopal, A. K.; Teitler, S.; Ngai, K. L. *J. Phys. C.* **1984**, *17*, 6611.
(61) Ngai, K. L.; Rajagopal, A. K.; Teitler, S. *Physica A (Amsterdam)* **1985**, *133A*, 359.
(62) Ngai, K. L.; Rajagopal, A. K.; Teitler, S., unpublished results; *Nucl. Phys. B (Suppl.)* Garrod, C., Ed.; in press.
(63) Kullback, S. *Information Theory and Statistics*; Wiley: New York, NY, 1959.
(64) Malhotra, B. D.; Pethrick, R. A. *Eur. Polym. J.* **1983**, *19*, 457; *Polym. Commun.* **1983**, *24*, 165.
(65) Curro, J. J.; Roe, R. *Polymer* **1984**, *25*, 1424.
(66) Victor, J. G.; Torkelson J. M. *Macromolecules* **1987**, *20*, 2241.
(67) Robertson, R. E. *Ann. N.Y. Acad. Sci.* **1981**, *371*, 21.
(68) Ngai, K. L.; Wang, C. H.; Fytas, G.; Plazek, D. L.; Plazek, D. J. *J. Chem. Phys.* **1987**, *86*, 4768.

Test of the Reptation Concept: Crystal Growth Rate as a Function of Molecular Weight in Polyethylene Crystallized from the Melt

John D. Hoffman* and Robert L. Miller*

Michigan Molecular Institute, 1910 W. St. Andrews Road, Midland, Michigan 48640.
Received December 28, 1987; Revised Manuscript Received March 18, 1988

ABSTRACT: The concept of reptation in high polymer melts is tested for the case of crystallization, where a strong force resulting from the free energy difference between the subcooled liquid and the lamellar crystal is envisaged as drawing a chain through a reptation tube onto the substrate. The presence of the strong force sets this process apart from the case of free curvilinear diffusion. The test is made by determining the dependence on molecular weight of the crystal growth rate at constant undercooling, $G_{\Delta T\text{const}}$. According to the development presented, which combines nucleation and reptation theory, $G_{\Delta T\text{const}}$ varies as $n^{-[y+f(\lambda)]}$, where the factor n^{-y} with $y = 1$ derives directly from the steady-state reptation concept where the overall friction coefficient in the tube is proportional to the number of monomer units n. The factor $f(\lambda)$ is of statistical mechanical origin and accounts for the free energy of first attachment of a chain to the substrate. On the basis of published growth rate data on 11 polyethylene fractions $n_z = 1590$ to $n_z = 14\,500$, it was determined that $y = 1.0 \pm 0.20$ in the vicinity of the regime I → II transition. This renders plausible the simple steady-state reptation tube model in this special application, where the molecule is reeled in quite rapidly allowing little time for lateral excursions of the tube, but not so rapidly that only short sections of "slack" can crystallize. Estimates are given for the reptation time. The paper contains results of interest concerning nucleation theory as it applies to chain-folded systems. Besides modifying the theory to account for the free energy of first attachment, the treatment is developed for regimes I and II along parallel lines first excluding the backward reaction, i.e., stem removal, in the "$\epsilon = 0$" case and then in the case denoted "$\epsilon = 1$" including it. The differences between the two are minimal, showing that neglect of the backward reactions is permissible under stated circumstances. It is significant that the improved theory (with either $\epsilon = 0$ or $\epsilon = 1$), coupled with improved input data, leads to a lower substrate completion rate g and a smaller substrate length ($L \simeq 210$ Å) than had been estimated previously.

I. Introduction

In its simplest form, the reptation concept proposed by de Gennes holds that under appropriate circumstances the overall friction coefficient of a linear polymer chain in the liquid state is proportional to its length.[1] Here we propose to test this idea by considerations based on the dependence on molecular weight of the rate of crystallization from the melt at constant undercooling.

At a fixed undercooling, the mean force $\bar{f}_c$ drawing the polymer molecule onto the growth front is constant av-

0024-9297/88/2221-3038$01.50/0

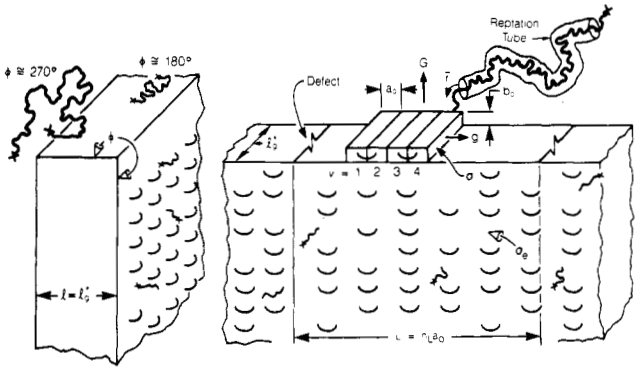

Figure 1. Details of model: molecular morphology.

eraged over time and the nucleation terms in the growth rate are also essentially constant. By straightforward reasoning one can predict from the elementary reptation model that at a constant undercooling the growth rate from the melt G will contain a factor n^{-1} where n is the number of chain units.[2,3] This comprises the most important factor in the dependence of G on chain length. (The n^{-1} factor arises from the fact that the "reeling in" rate $\bar{r}$ is proportional to $\bar{f}_c/\zeta n$ where ζ is the monomeric friction coefficient: in the elementary model, the motion of the molecule is strictly curvilinear and the molecule does not diffuse sideways from the reptation tube.) An additional though smaller contribution to the molecular weight dependence is of statistical mechanical origin and arises from the free energy change associated with the first attachment of a chain to the crystal surface. As will be outlined subsequently, this leads to a factor $n^{-\lambda}$ in the nucleation rate. The quantity λ is related to the angle of sweep ϕ of the initial (nucleating) molecule whose one end is attached to the surface (see Figure 1). Values of λ are restricted to the range $^1/_3$ to $^1/_2$, corresponding to $\phi = 270°$ and $\phi = 180°$, respectively. It will be shown that at a fixed undercooling ΔT, the growth rate as a function of the number of chain segments n in the vicinity of the regime I → II transition is of the form

$$G_{\mathrm{I,II}(\Delta T\mathrm{const})} \propto n^{-[y+f(\lambda)]} = n^{-s} \qquad (1)$$

where $y = 1$ for the steady-state reptation model mentioned above and where one expects $f(\lambda)$ to be $^1/_3$ to $^1/_2$ for regime I crystallization and $^1/_6$ to $^1/_4$ for regime II crystallization.

The quantity s in eq 1 is in principle experimentally accessible. If the experimentally determined s values are such that with reasonable values of λ the value $y \cong 1$ obtained, it would follow that the n^{-1} law arising from reptation was substantially correct in this application. We shall show that the experimental s values derived from published growth rate data[4] for 11 polyethylene fractions $M_z = 23\,320$ ($n_z = 1590$) to $M_z = 203\,600$ ($n_z = 14\,500$) crystallized from the melt are such that $y = 1.0 \pm 0.2$, suggesting that the basic steady-state reptation concept giving n^{-1} behavior applies quantitatively in this particular case. (An analysis based on M_w allows a similar value of y, but the standard deviation is significantly higher.) If because of the presence of solvent molecules a marked degree of sidewise motion of the chain had occurred, y would have been nearer $^1/_2$ ("sea snake" model of DiMarzio et al).[5] If only crystallization of short sections of "slack"[6] had occurred, the dependence of the growth rate on molecular weight would have been smaller.

The analysis of the growth rates to obtain s for the polyethylene fractions is carried out at fixed undercoolings on either side of the regime I → II transition, which occurs at $\overline{\Delta T} = 16.46 \pm 0.39$ °C. This allows one to be certain of the regime, and the equalities that hold at the I → II transition permit such quantities as the substrate completion rate g and the substrate length L to be estimated with some accuracy. (A meaningful estimate of g and L can only be made if the regime I → II transition is observed, and one is also more certain of the application of eq 1 under these conditions). The required I → II transition in polyethylene occurs in the molecular weight range mentioned above but becomes too diffuse at higher molecular weights.[4] Comments are given concerning situations where one must expect the model to fail. For example, the advent at sufficiently high molecular weights of a situation where most of the molecules are involved in multiple nucleation events is discussed, as is the onset of crystallization of "slack" at large undercoolings. The simple steady-state reptation concept has it that the entire pendant chain resists the force of crystallization, and this condition is not always attained.

We note now an important proviso concerning the application of eq 1 to real systems. The simple reptation tube model, which leads to the n^{-1} part of the behavior in eq 1, applies to a high molecular weight polymer melt. This model plays a major role in explaining how a long molecule can be readily extracted by the force of crystallization from its high molecular weight interentangled neighbors in the melt and thence crystallize in the chain-folded mode.[2,3,5] In its steady-state manifestation, where the overall friction coefficient is proportional to the chain length, the reptation model is not applicable to crystallization from concentrated or a dilute solution. In these latter cases considerable lateral motion is possible, and in one calculation[5] this gives an effective friction coefficient that varies as $n^{-1/2}$. This has special significance in the case of crystallization from the melt if the polymer fraction involved contains significant quantities of noncrystallizable low molecular weight material that is rejected at the growth front thus forming a low molecular weight liquid boundary layer. Owing largely to the work of Keith and Padden, this phenomenon is well-known[7-9] and leads to a situation where the act of crystallization actually occurs from a more or less concentrated solution rather than from a fully interentangled melt. Specimens of this type, seemingly typifying "melt crystallization", cannot be expected to obey eq 1 with $y \cong 1$. The proviso here is that in order to test for the presence of the reptation-based n^{-1} component in eq 1, the noncrystallizable low molecular weight molecules in the fraction must be removed prior to measuring the growth rate in the melt. We explicitly emphasize that this was done by prior precipitation from dilute xylene solution for the 11 polyethylene fractions analyzed in this study. As a result, we believe our test of the n^{-1} law to be a valid one.

The elementary reptation process envisioned here involves two simplifying features. The first is that the chain is essentially pinned at one end (crystal surface), and the second is that a relatively strong force $\bar{f}_c$ rather rapidly draws the chain through the reptation tube onto the crystal surface. This process is simpler than ordinary self-diffusion which occurs over a long period of time and which in recent treatments involves such effects as "tube renewal" at the chain ends and lateral excursions of the reptation tube.[10-13] In our view, crystallization experiments meeting the provisos set forth above may well approximate the conditions where the simple steady-state reptation tube concept approaches a considerable degree of physical reality.

The low values of s implied by data on other polymers given in the literature are noted and discussed. Estimates are given of the time required for drawing a molecule of

specified length onto the growth front using a value of the monomeric friction coefficient derived from self-diffusion and other data.

The combination of nucleation and reptation theory given previously is modified and simplified. Expressions for the growth rates in regimes I and II are derived on two bases, one where the backward reaction (stem removal) is supressed and the other where the backward reactions are assumed to be fully active. It is shown that the results are very similar; in particular, eq 1 is unaffected, which lends generality to the test of steady-state reptation. The newer and broader based theory, taken together with improved input data (particularly concerning the monomeric friction coefficient and activation energy associated with reptation), leads to improved results for the substrate completion rate g and the substrate length L for polyethylene. The smaller g and L values obtained here alleviate certain difficulties that had been encountered with earlier estimates.

II. Theory

Below we sketch out the development of expressions for the growth rates of a lamellar chain-folded high polymer in regimes I and II with special emphasis on obtaining the dependence of the growth rate on molecular weight (or more specifically the number of chain units n in a particular fraction) and on undercooling ΔT. The analysis refers to crystallization from the pure subcooled liquid state. Our strategy will be first to calculate the substrate completion rate g_{rept} from a proper combination of nucleation theory (which defines the mean force of crystallization) and the reptation approach. This will show the role of the total friction coefficient ζn of a chain of length $l_0 = nl_u$ in the crystallization process: here n is the number of monomer units in the chain, l_u the length of each monomer unit, and ζ the monomeric friction coefficient at the temperature of interest. The molecule in the subcooled liquid state that is reeled onto the substrate by the force of crystallization $\bar{f}_c$ is assumed to be pulled through a reptation tube consisting of its interentangled neighbors.[2,3,5] The resistance to the molecule being pulled onto the substrate in the steady-state case is given by ζn. This establishes the reeling rate $\bar{r}$ as $\bar{f}_c/\zeta n$, which is readily converted to g_{rept}, the substrate completion rate consistent with the steady-state reptation concept. The quantity g_{rept} will then be compared with g_{nuc}, the substrate completion rate as given by a modern version of nucleation theory. This establishes the proper molecular weight dependence of g_{nuc} and provides a method of estimating its absolute value. The nucleation rate i is then calculated. This includes a correction of statistical mechanical origin, which accounts for the free energy change on first attachment. The formulation of i and g allows expressions to be obtained for the observed growth rate in regimes I and II as a function of undercooling and molecular weight. For a constant undercooling, the calculations lead to eq 1. By application of eq 1 to experimental data, one can test the validity of the steady-state reptation concept, which gives the reptation component of the growth rate as varying as $1/n$; i.e., $y = 1$, for both regimes I and II. The key features of the model are shown in Figures 1 and 2.

We begin by estimating the mean force of crystallization $\bar{f}_c$. The free energy of formation of a surface patch is given by

$$\Delta\phi = 2b_0\sigma l - a_0b_0l(\Delta G) + \lambda kT \ln (l_0/x_0) - (\nu - 1)a_0b_0[l(\Delta G) - 2\sigma_e] \quad (2)$$

Here σ = lateral surface free energy, $\sigma_e = q/2a_0b_0$ = fold surface free energy, a_0 the stem width, b_0 the layer thickness, a_0b_0 the cross-sectional area of the chain, q the work of chain folding, and ν the number of stems added to the surface patch. The quantity l is the lamellar thickness, which is treated as a variable (see later). The quantity

$$\Delta G = \Delta h_f(\Delta T)/T_m \quad (3)$$

is the free energy of fusion. Here Δh_f is the heat of fusion, ΔT the undercooling $T_m - T$, T the isothermal crystallization temperature, and T_m the melting point appropriate to the molecular weight under consideration.

Equation 2 corresponds to the free energy of formation commonly employed[14] in nucleation theory for polymers, except that an additional term, $\lambda kT \ln (l_0/x_0)$, has been added to account for the entropy reduction associated with the attachment of the first ($\nu = 1$) stem. (The first three terms in eq 2 describe the net free energy of attachment of the first full stem; $2b_0\sigma l$ is the free energy associated with constructing the lateral surfaces involved, $a_0b_0l(\Delta G)$ is the corresponding free energy of fusion, and $\lambda kT \ln (l_0/x_0)$ is the free energy of attachment of the first chain.) The term $\lambda kT \ln (l_0/x_0)$, employed by one of us on an earlier occassion[4] but ordinarily not considered, is introduced here because it leads to a small but nevertheless important contribution to the molecular weight dependence of the crystallization rate at a fixed undercooling. In eq 2

$$\lambda = \pi/2\phi \quad (4)$$

where ϕ is the angle of sweep in radians of the first ($\upsilon = 1$) chain after it has achieved its first attachment (see Figure 1). The quantity l_0/x_0 is the effective statistical chain length.

The additional term involving λ is based on the calculation due to Lauritzen and DiMarzio[15] for the partition function of a polymer chain confined to a notch or corner of containment angle ϕ, the one end of the chain being attached along the intersection of the two planes that define the notch or corner. The partition function of the chain prior to attachment is $Q_i = Z^m$ where Z = partition function of a chain unit and m is the effective number of chain units; after attachment the partition function is $Q_f = Z^m/m^\lambda$, leading to a free energy change on attachment of $\Delta F = \lambda kT \ln m$. We employ $m = l_0/x_0$ where x_0 plays the role of a statistical chain length unit. (As mentioned above, one expects the angle of sweep for a polymer chain to be between $\phi = 270°$ and $\phi = 180°$ as depicted in Figure 1, giving λ values in the range $^1/_3$ to $^1/_2$). The correction involving $\lambda kT \ln (l_0/x_0)$ is applied only to the attachment of the first stem. Each "first" stem involves the attachment of a "new" molecule, but such "new" attachments are much less frequent during the substrate completion process. A correction for the change in the free energy resulting from the shortening of the pendant chain by an amount l_g^* that accompanies the addition of each stem during the substrate completion process has been omitted from eq 2; as will be shown subsequently, this correction is negligible.

In order to calculate the substrate completion rate using the reptation approach, it is required to know the force pulling on a molecule resulting from the free energy difference between the subcooled liquid and the lamellar crystal. From eq 2 one finds that the mean force associated with drawing in the chain is related to the slope of the $\Delta\phi$ vs ν plot (see heavy dots in Figure 2) according to the calculation of DiMarzio et al.:[5]

$$\bar{f}_c' = \frac{1}{l_g^*}\left[\frac{d(\Delta\phi)}{d\nu}\right] = -a_0b_0(\Delta G)\left(\frac{\delta}{l_g^*}\right) = -a_0b_0(\Delta G)\chi_c' \quad (5)$$

where we have used the relation[14]

$$l = \langle l \rangle = l_g^* = \frac{2\sigma_e}{\Delta G} + \delta \tag{6}$$

which is the flux-determined lamellar thickness that is readily derived from nucleation theory (see later). For the simple version of nucleation theory employed in the main text (denoted the "$\epsilon = 0$" case in which the backward reactions are supressed) one gets

$$\delta = kT/2b_0\sigma \tag{7}$$

The quantity δ must be greater than zero to allow the slope to be negative, i.e., to allow substrate completion. Commonly the value of δ is between roughly 5 and 10 Å. (The value of δ for the "$\epsilon = 1$" case where the backward reactions are assumed to be fully active is given in the Appendix.)

It is important to note that the factor $a_0b_0(\Delta G)$ in eq 5 is the force associated with a chain being drawn onto a very large crystal where surface effects are negligible. We take this to be representative of the force exerted on a chain during the zippering down of a stem in the absence of the effect of chain folds. No force is applied during formation of the fold. When the reptation process is treated in a somewhat more detailed manner below, we shall interpret the factor $\delta/l_g^* = \chi_c'$ in eq 5 as the fraction of time that the chain experiences the force $a_0b_0(\Delta G)$.

The "reeling in" rate $\bar{r}$ will be proportional to the mean force of crystallization divided by the overall friction coefficient ζn associated with the chain:[2,3,5]

$$\bar{r}_{rept} = \bar{f}_c/\zeta n \tag{8}$$

It is through the factor ζn that the concept of steady-state reptation (as opposed to reptation of short sections of "slack"[6]) enters nucleation theory.

Because the customary version of nucleation theory explicitly displays the work of chain folding q as the factor $\exp(-q/kT)$ in both $\bar{r}$ and g (see later), we follow an earlier treatment to obtain a form of $\bar{f}_c$ consistent with the model that contains this factor. We define a factor χ_c that represents the fraction of the time that the full force $a_0b_0(\Delta G)$ is pulling on the chain during stem formation:[2]

$$\chi_c = \frac{\tau_0(l_g^*/l_u)}{\tau_0(l_g^*/l_u) + \tau_0(l_f/l_u)e^{+q/kT}} \cong (l_g^*/l_f)e^{-q/kT} \tag{9}$$

where τ_0 is the time associated with attaching a monomer unit and l_f is the length of a fold. This time average approach leads to an alternative expression for the mean force

$$\bar{f}_c = -a_0b_0(\Delta G)\chi_c = -a_0b_0(\Delta G)\left(\frac{l_g^*}{l_f}\right)e^{-q/kT} \tag{10}$$

We shall employ eq 10 henceforth, taking care to keep χ_c' numerically equal to χ_c, i.e., $\bar{f}_c' = \bar{f}_c$, in the region of application, which will be in the vicinity of the regime I → II transition.

The negative sign in eq 5 and 10 simply means that the net force pulls the chain onto the crystal face in the undercooled system. It is henceforth omitted.

Though our main purpose is to develop the molecular weight (chain length) dependence of crystallization, we digress to examine in numerical terms the consequences of setting $\chi_c' = \chi_c$. Equation 10 and expressions derived from it will be employed in analysis of data mainly at the I → II regime transition, i.e., at $\overline{\Delta T}_{I\to II} = 16.46$ °C in polyethylene fractions. Here $l_g^* \cong 169 \times 10^{-8}$ cm from eq 6 with $\sigma_e = 90$ erg cm^{-2}, $T_m = 418.1$ K (giving $T = 401.7$ K), $\Delta h_f = 2.8 \times 10^9$ erg cm^{-3}, and $\delta = 5.66 \times 10^{-8}$ cm from eq 7 with $b_0 = 4.15 \times 10^{-8}$ cm and $\sigma = 11.8$ erg cm^{-2}. (The melting point $T_m = 418.1$ K corresponds to that of the fraction $n_z = 14\,500$, which is the specimen of highest molecular weight that exhibits a clear-cut regime I → II transition[4]). The value of q is 4900 cal/mol of folds.[4] With these input data one estimates that $\chi_c' \cong 0.0336$ and from setting $\chi_c' = \chi_c$ that $l_f = 10.86 \times 10^{-8}$ cm, suggesting a fold with ~8–9 $-CH_2-$ units. This is a reasonable value for the length of a fold, justifying eq 10 in numerical terms.

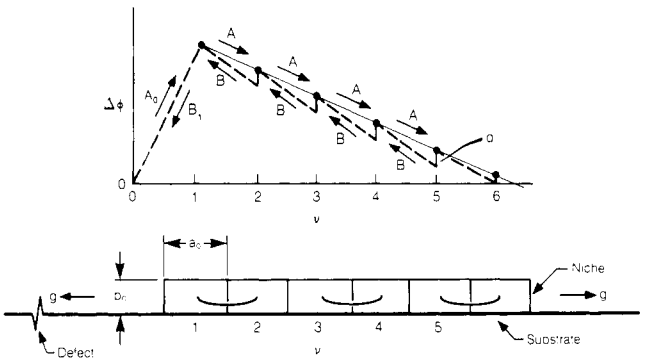

Figure 2. Details of model: barrier system and its relation to molecular morphology.

Proceeding with the reptation approach, we find the mean "reeling in" rate to be

$$\bar{r}_{rept} \equiv \bar{f}_c/\zeta n = \frac{a_0b_0(\Delta G)(l_g^*/l_f)e^{-q/kT}}{\zeta_0 n} e^{Q_D^*/RT_0}e^{-Q_D^*/RT} \tag{11}$$

where we have used

$$\zeta = \zeta_0 e^{-Q_D^*/RT_0}e^{Q_D^*/RT} \tag{12}$$

to account for the temperature dependence of the friction coefficient. Here T_0 is a reference temperature in the melt, which for practical reasons we take to be 450 K for polyethylene, and ζ_0 is the monomeric friction coefficient at that temperature. The quantity Q_D^* is the activation energy of reptation in the melt, whose value for linear polyethylene is taken to be known from the tracer diffusion experiments of Fletcher and Klein[16] ($Q_D^* \cong 5736$ cal mol^{-1}).

It is now possible to find the substrate completion rate implied by the reptation-based model. From Figure 1 one sees that $g_{rept} = \bar{r}(a_0/l_g^*)$. Accordingly

$$g_{rept} \equiv \bar{r}\left(\frac{a_0}{l_g^*}\right) = \frac{a_0}{n}\left[\frac{a_0b_0(\Delta h_f)\exp(Q_D^*/RT_0)}{\zeta_0 l_f}\right]\left(\frac{\Delta T}{T_m}\right)e^{-Q_D^*/RT}e^{-q/kT} \tag{13}$$

The foregoing is now compared to the substrate completion rate from the nucleation approach. For the simplest "$\epsilon = 0$" case, which supresses the backward reaction

$$g_{nuc} \equiv a_0A = a_0\beta e^{-q/kT} \tag{14}$$

where the forward reaction in the substrate completion process (see Figure 2) is given by the customary expression[14]

$$A = \beta e^{-q/kT} \tag{15}$$

Here β is a retardation factor in events per second expressing the resistance to transport of segments to the growth front and $\exp(-q/kT)$ represents the retardation resulting from the necessity of forming a chain fold. Combination of eq 13 and 14 gives

$$\beta = \frac{1}{n}\left[\frac{a_0b_0(\Delta h_f)\exp(Q_D^*/RT_0)}{\zeta_0 l_f}\right]\left(\frac{\Delta T}{T_m}\right)e^{-Q_d^*/RT} \tag{16}$$

This connects the two approaches. The quantity in braces is a frequency factor on the order of 3×10^{13} events/s for polyethylene. The free energy change on attachment of a stem in the substrate completion process is of the form $\lambda kT\{\ln(\bar{l}_0/x_0) - \ln[(\bar{l}_0 - l_g^*)/x_0]\}$ where $\bar{l}_0$ is the average length of the pendant chain. This leads to $A = [(\bar{l}_0 - l_g^*)/\bar{l}_0]^{\lambda\beta} \exp(-q/kT)$. The factor $[(\bar{l}_0 - l_g^*)/\bar{l}_0]^{\lambda}$ is always very close to unity and may be safely neglected. We therefore retain eq 14 and 15 as they stand in the rest of the treatment.

The retardation factor β in this particular formulation actually contains two physical entities. It expresses the retardation resulting from reptation through n^{-1}, ζ_0, and Q_D^*, and also it expresses the effect of the free energy driving force through the factor $\Delta h_f(\Delta T)/T_m$.

It is convenient for further developments to simplify the notation by defining β as

$$\beta = \left(\frac{\kappa}{n}\right)\left(\frac{kT}{h}\right)\left(\frac{\Delta T}{T_m}\right)e^{-Q_D^*/RT} \tag{17a}$$

where

$$\kappa = \left(\frac{h}{kT}\right)\left[\frac{a_0 b_0(\Delta h_f)\exp(Q_D^*/RT_0)}{\zeta_0 l_f}\right] \tag{17b}$$

We now estimate the numerical value of κ. For the case of the polyethylene fraction at the regime I → II transition temperature $T_{I\to II} = 401.7$ K and with the cross-sectional area of the chain $a_0 b_0$ set at 18.88×10^{-16} cm, the heat of fusion Δh_f at 2.8×10^9 erg cm^{-3}, $l_f = 10.86 \times 10^{-8}$ cm as described above, and $Q_D^* = 5736$ cal mol^{-1}, one finds the numerical value of κ to be

$$\kappa \cong 3.5_6 \times 10^{-9}/\zeta_0 \tag{18}$$

where ζ_0 is the monomeric friction coefficient in erg s cm^{-2} at the reference temperature $T_0 = 450$ K.

The monomeric friction coefficient for polyethylene in the melt state is less certain than the other input data but can still be bounded rather closely. At 450 K, Pearson's expression[17] based on viscosity data gives $\zeta_0 \cong 2.2 \times 10^{-9}$ erg s cm^{-2}. The method of DiMarzio et al,[5] as corrected for the length of chain in the tube as mentioned by Flory and Yoon[18] based on the reptation treatment of Klein and Ball,[6] gives $\zeta_0 \cong 0.93 \times 10^{-9}$ erg s cm^{-2} at the same reference temperature; a value of $\zeta_0 \cong 1.2 \times 10^{-9}$ erg s cm^{-2} at 450 K is estimated by applying the Rouse expression to the viscosity of low molecular weight polyethylene melts below the critical molecular weight.[18,19] Here and elsewhere we shall employ the value $\zeta_{0(450K)} \cong 10^{-9}$ erg s cm^{-2}. This may be taken to be correct to within a factor of about 2. From eq 18, κ in eq 17a is ~3.6 to the same accuracy. This establishes the absolute value of the preexponential part of the retardation factor β.

Having found the approximate value of κ in eq 17a, it is of interest to estimate the actual value of g and $\bar{r}$ for the case of polyethylene. From eq 14 and 17a one arrives at the practical formula

$$g = a_0\left(\frac{\kappa}{n}\right)\left(\frac{kT}{h}\right)\left(\frac{\Delta T}{T_m}\right)e^{-Q_D^*/RT}e^{-q/kT} \tag{19}$$

At $T_{I\to II} = 128.5$ °C = 401.7 K, $\Delta T_{I\to II} = 16.46$ °C, and $a_0 = 4.55 \times 10^{-8}$ cm one finds with $\kappa = 3.6$ the substrate completion rate

$$g\ (\text{cm s}^{-1}) = \frac{8.77 \times 10^{-2}}{n} \tag{20}$$

which gives 5.5×10^{-5} cm s^{-1} for $n = 1590$ (MW = 22 320) and 6.0×10^{-6} cm s^{-1} for $n = 14\,500$ (MW = 203 600). The corresponding "reeling in" rate from eq 13 is

$$\bar{r}\ (\text{cm s}^{-1}) = g(l_g^*/a_0) = \frac{3.2}{n} \tag{21}$$

which gives 2.0×10^{-3} cm s^{-1} for $n = 1590$ and 2.2×10^{-4} cm s^{-1} for $n = 14\,500$. Both g and $\bar{r}$ are roughly an order of magnitude lower than our earlier estimates.[20] Most of the reduction results from the larger friction coefficient employed in the current estimate (10^{-9} vs 3.56×10^{-10}, erg s cm^{-2}) and the lower Q_D^* (5736 vs 7000 cal mol^{-1}). The molecular weight range mentioned above corresponds to the extremes of n_z that will subsequently be utilized to determine s and thence y for polyethylene.

One important consequence of the lower estimates of g and $\bar{r}$ is that the substrate length L to be discussed later is decidedly smaller than we had estimated in previous work. It will be shown that the new result of $L \simeq 210$ Å is considerably more satisfactory.

As an aid in the understanding of the nature of the test of reptation theory to be given here, we employ eq 21 to estimate the mean time required to draw an entire molecule of a given length onto the growth front. The relevant expression, which accounts for the fact that the velocity increases as the length of the molecule remaining in the melt decreases and which also allows for the time for fold formation, is[20]

$$t_{rept}\ (\text{s}) = \tfrac{1}{2}\left(\frac{l_0}{\bar{r}}\right) = \tfrac{1}{2}\left(\frac{l_u n}{\bar{r}}\right) = 1.9 \times 10^{-9} n^2 \tag{22}$$

with $l_u = 1.27 \times 10^{-8}$ cm and where eq 21 has been used for $\bar{r}$. The above expression yields $t_{rept} = 4.9 \times 10^{-3}$ s for $n = 1590$ and 0.41 s for $n = 14\,500$. The results apply at $\overline{\Delta T} = 16.46$ °C for polyethylene, i.e, at the regime I → II transition.

The above calculations assume that if a chain is interrupted by another (i.e. "strange") molecule entering the "niche" the dangling chain of the original molecule finds another "niche" in a time which is short compared to that required to form a fold, the latter being $\tau_0(l_f/l_u)\exp(q/kT)$ as expressed in eq 9. With $\chi_c = 0.0336$ from eq 9, one finds the time required to form a fold is close to $1/\chi_c$ or ~30 times longer than that needed to put down a single stem of length l_g^*. Thus it appears that the delay time associated with fold formation provides considerable opportunity for a dangling chain to find a niche. Of course the dangling chain of an "original" molecule that is interrupted by a "strange" molecule will form an amorphous traverse to its new niche, and this traverse will contribute to the amorphous component of the polymer. This new niche may be in the same lamella or sometimes on an adjacent lamella so that the chain forms an interlamellar link (see discussion in the vicinity of eq 41).

The short reptation times quoted above are entirely compatible with the estimated force of crystallization and the monomeric friction coefficient and establish that steady-state reptation is rapid enough near the regime I → II transition in polyethylene to allow substantial chain folding at the undercooling cited. (At lower crystallization temperatures in regime III only sections of "slack" can be drawn onto the growth front, but at the higher temperature regime I → II transition the crystallizing system experiences essentially the full length of the dangling molecule over the molecular weight range mentioned,[2] as our result that $y \cong 1$ to be obtained subsequently will show). Eq 22 implies that the longer molecules in the distribution in a given fraction will have the strongest influence on the reptation time. It will emerge that the best fit of the

growth rate data corresponds to $n = n_z$ where $n_z = M_z/14.03$.

An important consequence of the relatively short reptation times calculated with eq 22 is that in the limited time available one expects relatively little lateral motion of the tube itself. This differentiates the reptation process in the case of crystallization from that occurring in "free" curvilinear self-diffusion in a polymer melt where much longer times are required for a molecule to move a distance equal to its full contour length. In the case of melt crystallization in the molecular weight range mentioned, one does not expect major perturbations from such effects as lateral excursions of the reptation tube.

Below we give a simplified yet adequate version of the growth rates in regimes I and II, which is designed to illuminate the origin of the dependence of these growth rates on chain length. (The growth rates in regimes I and II are observable quantities.) We consider crystallization from the melt only and specifically exclude from consideration any system containing significant amounts of noncrystallizable low molecular weight material.

It is sufficient for our purpose to consider the forward reactions only, i.e., the case referred to earlier as "$\epsilon = 0$". This approach is justified as a reasonable hypothesis by the fact that recent careful simulations by Guttman and DiMarzio[21] have shown that regimes I, II, and III can be reproduced by considering forward reactions only and by the fact that physical arguments to be noted later are sufficient to imply that the backward reactions (stem removal) are relatively inactive in high polymeric systems at moderate and large undercoolings. We deem it fully reasonable to suppose that the backward reaction is almost completely inactive in regime III and suppose further that the backward reactions may well be muted near the regime I → II transition. While the question of the degree of activity of the backward reactions at moderate and large undercoolings is one of fundamental physical interest, it does not lead to difficulties in the present application. Expressions for all quantities of interest, including the temperature and chain length dependence of crystal growth in regimes I and II, are given in the appendix for the case "$\epsilon = 1$", where the backward reactions (stem removal processes) are treated in the conventional way and assumed to be fully active. There is no significant difference between the "$\epsilon = 1$" and "$\epsilon = 0$" cases in the present application; in particular, eq 1 is found in each instance.

Consider now the nucleation rate. The barrier system is depicted in Figure 2. In the "$\epsilon = 0$" case we set $B_1 = B = 0$. For the rate of attachment of the first ($\nu = 1$) stem in stems per second we therefore write

$$A_0 = \beta e^{-2b_0\sigma l/kT} e^{-\lambda \ln(l_0/x_0)} \tag{23}$$

$$A_0 = \beta (x_0/l_0)^\lambda e^{-2b_0\sigma l/kT}$$

$$A_0 = \beta (x_0/l_u)^\lambda (1/n^\lambda) e^{-2b_0\sigma l/kT}$$

where β is given by eq 17. The quantity $2b_0\sigma l$ is the free energy required to form the first full stem with a "niche" that invites substrate completion without further cost involving σ, and $\lambda kT \ln (l_0/x_0)$ is the free energy of first attachment of the primary chain. The net nucleation rate is given by

$$i \text{ (nuclei s}^{-1}\text{ cm}^{-1}) \equiv S_T/L = S_T/n_L a_0 \tag{24a}$$

where the total flux S_T is[14]

$$S_T = \frac{1}{l_u}\int_{2\sigma_e/(\Delta G)}^{\infty} N_0 A_0 \, dl \tag{24b}$$

In the above L is the substrate length $n_L a_0$, n_L being the number of stems of width a_0 that comprise the substrate. The lower bound of integration in (24b) corresponds to the thinnest possible lamella, i.e., one that is just on the point of melting.[14] The number of reacting species is taken as proportional to the substrate length according to[2,22]

$$N_0 = C_0 n_L \tag{24c}$$

Here C_0 is a large number whose principal component represents the configurational path degeneracy associated with the nucleation process—the crystal surface has numerous molecules with initial attachments, each with many configurations which have the possibility of ultimately leading to a first full stem. The value of C_0 can be estimated from experiment (see later). The above yields

$$i \text{ (nuclei cm}^{-1}\text{ s}^{-1}) = C_0\beta(x_0/l_u)^\lambda (1/n)^\lambda (1/a_0)\left(\frac{kT}{2b_0\sigma l_u}\right) e^{-4b_0\sigma\sigma_e/(\Delta G)kT} \tag{25}$$

In regime I, which occurs at the highest observable growth temperatures, one surface nucleus causes the addition of a layer of thickness b_0 over a substrate length or "persistence length" $L = n_L a_0$ and leads to a growth rate equal to $b_0 iL$.[23-25] From eq 17a and (25) the growth rate in regime I is

$$G_I \text{ (cm s}^{-1}) \equiv b_0 iL = b_0 i n_L a_0 = \left(\frac{Z_{I(\lambda)}}{n^{1+\lambda}}\right)(\Delta T) e^{-Q_D^*/RT} e^{-K_{g(I)}/T(\Delta T)} \tag{26a}$$

where

$$Z_{I(\lambda)} = C_0 \kappa n_L (x_0/l_u)^\lambda \left(\frac{b_0 kT}{h}\right)\left(\frac{kT}{2b_0\sigma l_u}\right)\left(\frac{1}{T_m}\right) \tag{26b}$$

$$K_{g(I)} = \frac{4b_0\sigma\sigma_e T_m}{\Delta h_f k} \tag{26c}$$

Values of $Z_{I(\lambda)}$ and $K_{g(I)}$ can be obtained from experiment from plots of $\ln G + Q_D^*/RT - \ln \Delta T$ vs $1/T(\Delta T)$.

Regime II, which occurs at lower temperatures than regime I, involves multiple nucleation on the substrate of length L. The multiple nucleation is caused by the increased nucleation rate. The growth rate is equal to[23-25] $b_0(2ig)^{1/2}$. From eq 17a, 19, and 25 the growth rate in regime II is then

$$G_{II} \text{ (cm s}^{-1}) \equiv b_0(2ig)^{1/2} = \left(\frac{Z_{II(\lambda)}}{n^{1+\lambda/2}}\right)(\Delta T) e^{-Q_D^*/RT} e^{-K_{g(II)}/T(\Delta T)} \tag{27a}$$

where

$$Z_{II(\lambda)} = C_0^{1/2} \kappa (x_0/l_u)^{\lambda/2}\left(\frac{b_0 kT}{h}\right)\left(\frac{kT}{b_0\sigma l_u}\right)^{1/2}\left(\frac{1}{T_m}\right) e^{-q/2kT} \tag{27b}$$

$$K_{g(II)} = \frac{2b_0\sigma\sigma_e T_m}{(\Delta h_f)k} \tag{27c}$$

Numerical values of $Z_{II(\lambda)}$ and $K_{g(II)}$ can be obtained from experiment. The units of $Z_{I(\lambda)}$ and $Z_{II(\lambda)}$ are cm s^{-1} deg^{-1} and of $K_{g(I)}$ and $K_{g(II)}$ are deg^2.

The regime I → II transition, where G_I is equal to G_{II} at $\Delta T_{I\to II}$, is readily apparent in plots of log G vs T_x or ΔT for polyethylene fractions in the molecular weight range discussed here.[4,14] The regime I → II effect is particularly conspicuous in plots of $\ln G + Q_D^*/RT - \ln(\Delta T)$ vs $1/T(\Delta T)$, which exhibit two intersecting straight lines with

a slope difference close to two as required by eq 26 and 27.[4,14] The regime I → II effect is known not only in polyethylene crystallized from the melt[4] but in polyethylene single crystals formed from dilute solution[26] as well. It is also known in other melt-crystallized polymers, including poly(L-lactic acid),[27] poly(*cis*-isoprene),[28] and poly(1,3-dioxolane).[29] The type of treatment given here features a finite substrate length L and a substrate completion process following upon primary nucleation that is facilitated by the presence of a continuously regenerated full "niche" of mean length l_g^* that eliminates the need for forming a new lateral σ-type surface on stem addition. It is the only one extant that predicts both the existence and detailed behavior of the regime I → II transition. Calculations where nucleation is assumed to involve only deposition of partial stems do not appear to yield a regime I → II transition.

We mention in passing that the nucleation and growth model employed here, as typified in Figure 1 and 2, leads in a natural way to a regime II → III transition[30] at a temperature below the regime I → II transition where the niche separation between two nuclei approaches the dimensions of the stem width a_0: in regime III, $G_{III} \propto i$. The regime II → III transition has been observed in polyethylene,[30] poly(oxymethylene),[30,31] poly(pivalolactone),[32] *it*-polypropylene,[33] poly(3-hydroxybutyrate),[34] poly(*p*-phenylene sulfide),[35] and poly(*cis*-isoprene).[28] This provides additional verification of the general model.

Equations 26 and 27 provide the desired opportunity to examine the molecular weight dependence of the growth rate and thence the validity of the steady-state reptation concept which predicts $\beta \propto n^{-1}$. Specifically, at a constant undercooling ΔT (which for moderate to high molecular weights implies a nearly constant growth temperature T) the theory states that

$$G_{I(\Delta T\text{const})} \propto n^{-(1+\lambda)} = n^{-s_I} \tag{28}$$

$$G_{II(\Delta T\text{const})} \propto n^{-(1+\lambda/2)} = n^{-s_{II}} \tag{29}$$

Noting that s_I and s_{II} can be determined directly from the growth rate curves, one readily sees that y in

$$\beta \propto n^{-y} \tag{30}$$

can be determined as follows:

$$\text{regime I:} \quad y = s_I - \lambda \tag{31}$$

$$\text{regime II:} \quad y = s_{II} - \lambda/2 \tag{32}$$

If the steady-state reptation model is correct in this application, one should find $y \cong 1$.

A small correction resulting from the infrequent attachments of "new" molecules in the substrate completion process has been neglected in eq 29 and 32. This causes the term involving λ in these expressions for regime II to be slightly greater than $\lambda/2$, but this effect can safely be neglected in the present application, where the scatter of the data is considerably larger than the correction itself.

It is pertinent to discuss the expected range of validity of the treatment. We would apply the treatment in its present form only above the entanglement limit, where it is reasonable to propose a reptation tube. Further, we would only apply it in the case where there was no serious degree of multiple nucleation of a given molecule on different lamellae or excessive multiple nucleation on the same lamella, which would mute the n^{-1} dependence on molecular weight. Thus we would not attempt application in regime III where multiple nucleation is pervasive[30] and only reptation of "slack" occurs,[2] nor would we expect the treatment to apply above a certain high molecular weight. It will emerge that the latter departure occurs in polyethylene fractions somewhat above $M_z = 203\,600$; i.e., $n_z = 14\,500$. Finally, we repeat here the necessity of considering only specimens where the low molecular component has been removed, so that one deals with a relatively fixed reptation tube which gives $\beta \propto n^{-1}$; if low molecular weight "solvent" molecules are present, crystallization takes place at a boundary that corresponds to a concentrated solution where in the limiting case DiMarzio et al.[5] have shown that $\beta \propto n^{-1/2}$.

Before proceeding to analyze the molecular weight dependence of the growth rate data for the polyethylene fractions to estimate y, a number of issues are worthy of comment. The first of these is that the experimentally determined preexponential factors $Z_{I(\lambda)}$ and $Z_{II(\lambda)}$ in eq 26b and 27b, respectively, can be used to estimate n_L and thence the substrate length $L = n_L a_0$. By eliminating C_0 from eq 26b and 27b one finds that

$$n_L = 2\kappa \left(\frac{b_0 kT}{h}\right)\left(\frac{1}{T_m}\right)\left(\frac{Z_{I(\lambda)}}{Z_{II(\lambda)}^2}\right) e^{-q/kT} \tag{33}$$

at the regime I → II transition. The quantity $Z_{I(\lambda)}/Z_{II(\lambda)}^2$ for polyethylene is ~ 3.53 cm^{-1} s deg (see later). With $\kappa \cong 3.6$ estimated earlier it is found that $n_L \cong 45.6$ stems at $T_{I\to II} = 401.7$ K, leading to a value of $L = n_L a_0 \simeq 210$ Å within a factor of about 2. This is considerably smaller than earlier estimates, which ranged from ~ 1100 Å^2 to 0.77 μm,[22] and even ~ 5 μm[4] in a first attempt. The new estimate is certainly more accurate, being based on better values of Q_D^* and ζ_0 as well as a more refined if simpler theory.

The new smaller value of $L \simeq 210$ Å is significant. It removes an objection due to Point et al.[36] who noted that if L was actually as large as some of the earlier estimates, nonlineal growth should be readily observed. They failed to observe such an effect in polyethylene crystals formed in dilute solution and criticized nucleation theory on this account. With the small L derived here, one does not expect readily to observe accelerated (nonlineal) growth. (Growth would be nonlineal in time and of an accelerating character if the substrate length was equivalent to the edge of perimeter of a growing crystal.) The substrate length inferred here is definitely far smaller than the edge of all but the very smallest polymer crystals and is consistent with the aforementioned failure to observe nonlineal and accelerated growth. We note further that Point et al. criticized our previous estimates of g as being far too large and in a somewhat involved argument placed an upper limit on g of roughly 10^{-5} cm s^{-1}. Our new estimates of g based on eq 20 straddle this limit, so this objection now appears to be resolved as well. These developments place the kinetic theory of chain-folded growth in an improved position.

We observe in passing that the value of C_0 in eq 26b and 27b, as calculated with numerical values of $Z_{I(\lambda)}$ and $Z_{II(\lambda)}$ for polyethylene to be quoted subsequently, turns out to be $\sim 2.5 \times 10^7$. This shows the presence of the expected large configurational path degeneracy implied by the presence of many polymer chains attached with one or a few segments to the substrate (each with numerous configurations resulting from the chain character of the molecules), any one of which could potentially lead to an aligned stem, i.e., a nucleus at $\nu = 1$. A smaller C_0 is to be expected for polymers with stiff chains or chains with hard segments interspersed by flexible bonds.

Another issue involves the fact that we have in the main text deliberately omitted the effect of the backward (stem removal) process in nucleation and substrate completion

(the so-called "$\epsilon = 0$" case). This not only simplified the exposition but also embodied what we deem to be a reasonable physical approximation for moderate to large undercoolings. We were fortified in this view by the work of Guttman and DiMarzio,[21] who showed that the entire range of regime I, II, and III behavior could be modeled in detail in the complete absence of the backward reactions. To this we can add a physical argument. One may think of the process of stem removal at moderate and large undercoolings as akin to the desorption of a polymer molecule from a surface, the latter process being known to be slow.[37] The slowness of the desorption process is a result of the fact that *all* the chain segments must *simultaneously* depart the surface, which can be viewed as a statistically improbable event if the time alloted is short. It does not seem reasonable to require a fully active backward reaction in regime III, where the crystallization process takes place predominantly by acts of surface nucleation, and which on a per stem basis occurs on a very short time scale. On the other hand, backward reactions, as for $\epsilon = 1$, are in fact required at and very near the melting point where the time scale is very long and where in any case the principle of detailed balance must apply. We have, however, employed the "$\epsilon = 0$" approach only at moderate to large undercoolings ($\Delta T \geq \sim 13$ °C) in the case of polyethylene. Stated another way, we do not consider detailed balance (microscopic reversibility) as necessarily fully operative at such large undercoolings.

The problem of whether one should apply expressions based on "$\epsilon = 0$" or "$\epsilon = 1$" is relatively unimportant in the present instance where our main interest is in the molecular weight dependence of the growth rate in regimes I and II, for if the backward reactions are included, the key relations (28) through (32) are unchanged. The theory for G_{I}, G_{II}, κ, L, and other quantities for the case "$\epsilon = 1$", which assumes fully active backward reactions, is outlined in the Appendix. The results for the case $\epsilon = 0$ and $\epsilon = 1$ are remarkably similar.

Lastly we mention that the flux-determined value of l_g^* given earlier as eq 6 and 7 is derived from

$$\langle l \rangle = l_g^* = \frac{1}{l_u}\int_{2\sigma_e/\Delta G}^{\infty} lS(l)\,\mathrm{d}l \Big/ \frac{1}{l_u}\int_{2\sigma_e/\Delta G}^{\infty} S(l)\,\mathrm{d}l \qquad (34)$$

where $S(l) = N_0A_0$ for the "$\epsilon = 0$" case with A_0 being given by eq 23. The general formula for $S(l)$, which is applied in the Appendix to the "$\epsilon = 1$" situation is[25] $S(l) = N_0A_0(A - B)/(A - B + B_1)$, where the meaning of the variables A_0, A, B, and B_1 is shown in Figure 2.

III. Analysis of Growth Rate Experiments To Determine s and Estimate y in $\beta \propto n^{-y}$

We shall refer here to the extensive growth rate data on polyethylene fractions given in ref 4. All 11 fractions were first precipitated as single crystals from dilute xylene solution and then filtered while hot to remove low molecular weight material. The fractions were then carefully dried at 50 °C under vacuum, melted between cover slips, and spherulite and axialite growth rates measured under isothermal conditions. The reduced number of heterogeneities resulting from the filtration step allowed large and distinct spherulites or axialites to form, which in turn permitted accurate growth rates to be determined by optical microscopy. At the highest growth temperatures in regime I, the crystallization appeared in the form of axialites in the molecular weight range of interest here; at the lower temperatures in regime II, coarse-grained, nonbanded spherulites were formed.[4] Growth rates refer to the 110 facet.

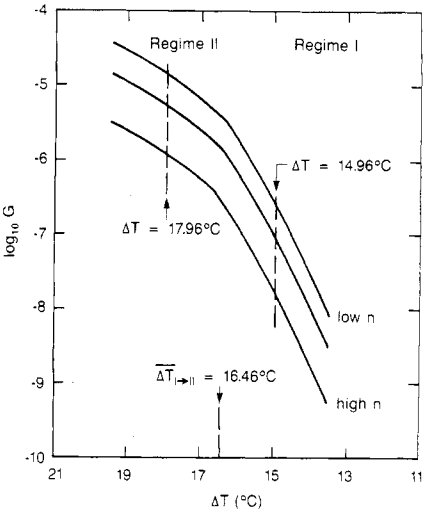

Figure 3. Plot of logarithm of growth rate as a function of undercooling ΔT (schematic). The experimental growth rates for various n_z at a constant ΔT (vertical dashed lines) are utilized in Figure 4 to construct plots of log $G_{\Delta T\mathrm{const}}$ vs log n_z for regimes I and II.

In general accord with eq 26 and 27 the 11 polyethylene fractions $n_z = 1590$ to $n_z = 14\,500$ give growth rate curves of the type shown schematically in Figure 3. The regime I → II transition was readily apparent in all of them. The temperature $T_{\mathrm{I}\to\mathrm{II}}$ where the growth rates in regimes I and II were equal for each fraction was known directly from experiment. The undercooling at the I → II regime transition, $\Delta T_{\mathrm{I}\to\mathrm{II}}$, was determined for each fraction as $T_m - T_{\mathrm{I}\to\mathrm{II}}$. The value of T_m for each fraction was determined by using the Flory–Vrij expression[38] in the form

$$T_m = T_m^0\left[\frac{n - 2.093}{n + 0.565[2.45 + R\ln n - 0.5n(1 - T_m/T_m^0)]}\right] \qquad (35)$$

with $T_m^0 = 418.7$ K (145.5 °C) on the basis of $n = M_w/14.03$. We found the mean value of the undercooling at the I → II regime transition to be $\overline{\Delta T}_{\mathrm{I}\to\mathrm{II}} = 16.46 \pm 0.39$ °C. The relatively constant $\Delta T_{\mathrm{I}\to\mathrm{II}}$ with molecular weight is consistent with eq 26 and 27 provided that n_L is constant, as is to be expected. Values of T_m and $\Delta T_{\mathrm{I}\to\mathrm{II}}$ for each fraction are given in Table I.

The growth rate data in the original source work[4] were expressed in the form of equations where T_m^0 was taken to be 419.7 K (146.5 °C) and which employed a different form of an effective Q_D^*. Using these original expressions for $G_{\mathrm{I(expt)}}$ and $G_{\mathrm{II(expt)}}$, the growth rate data were regenerated at temperatures corresponding to undercoolings of $\Delta T = 14.96$ °C for regime I and $\Delta T = 17.96$ °C for regime II, which corresponds to undercoolings exactly 1.5 °C above and below the regime I → II transition at $\overline{\Delta T} = 16.46$ °C. The melting points T_m employed in calculating the actual temperatures of crystallization are given in Table I. This procedure accurately reproduces the experimentally measured growth rates at the actual temperatures involved. The growth rates for each fraction at the undercoolings indicated above are listed in Table I and will be used below to estimate y.

The regenerated growth rate data were reanalyzed in the form of eq 26a and 27a assuming $K_{g(\mathrm{I})} = 2K_{g(\mathrm{II})}$ on the basis $T_m^0 = 418.7$ K = 145.5 °C and $Q_D^* = 5736$ cal mol^{-1} and with eq 35 to account for the reduction in T_m caused by finite molecular weight. The results are expressed in eq 39 and 40 to follow. The value of $K_{g(\mathrm{I})} = 1.91 \times 10^5$ deg^2

Table I
Molecular Weight, Melting Points, and Crystallization Properties of the Polyethylene Fractions

M_w	M_z	n_z	T_m (°C)[a]	$\Delta T_{I\to II}$ (°C)	G_I (cm s^{-1}) at ΔT = 14.96	G_{II} (cm s^{-1}) at ΔT = 17.96
18 100	28 000	2000	142.43	17.23	1.92×10^{-7}	1.58×10^{-5}
19 800	22 320	1590	142.68	16.48	1.40×10^{-7}	6.73×10^{-6}
24 600	27 720	1980	143.19	16.79	1.77×10^{-7}	9.96×10^{-6}
30 000	35 420	2520	143.58	16.18	2.92×10^{-7}	5.99×10^{-6}
30 000[b]	35 420	2520	143.58	16.18	2.22×10^{-7}	3.68×10^{-6}
30 600	38 360	2740	143.61	16.41	1.23×10^{-7}	8.74×10^{-6}
37 600	43 820	3120	143.94	16.64	2.49×10^{-7}	3.33×10^{-6}
42 600	53 480	3810	144.11	16.11	1.43×10^{-7}	4.45×10^{-6}
62 800	98 560	7030	144.54	16.14	3.87×10^{-8}	1.43×10^{-6}
68 600[c]			144.62	16.62		
74 400	85 960	6130	144.68	15.88	4.03×10^{-8}	9.48×10^{-7}[d]
115 000	203 600	14500	144.97	16.87	1.27×10^{-8}	7.37×10^{-7}

$\overline{\Delta T}$ = 16.46 ± 0.39

[a] Calculated from Flory–Vrij expression, eq 35. [b] Two portions of this sample were run independently beginning with separate crystallization and filtration steps. [c] M_z not available for this fraction. [d] Because of excessive departure from eq 40, this growth rate was omitted when calculating the standard deviation of 41% for regime II quoted in the text.

and $K_{g(II)} = 0.955 \times 10^5$ deg^2 were employed. Through eq 26c and 27c this gives

$$\sigma\sigma_e = 1063 \text{ erg}^2/\text{cm}^4 \tag{36}$$

which with $\sigma_e = 90$ erg cm^{-2} yields

$$\sigma = 11.8 \text{ erg cm}^{-2} \tag{37}$$

This justifies the value of σ employed in previous calculations.

The nature of the determination of s from eq 28 and 29 is shown schematically in Figure 3. Selecting a fixed ΔT, say 14.96 °C in regime I, which is exactly 1.5 °C above $\overline{\Delta T}_{I\to II}$ = 16.46 °C, one then plots log G_I vs log n_z for the 11 specimens. Values of G_I at ΔT = 14.96 °C are listed in Table I. The slope, $-d \log G/d \log n_z$, is s_I and is listed in Table II. The process was repeated by using ΔT = 17.96 °C (1.5 °C below the I → II transition) for regime II and the resulting s_{II} given in Table II. The plots of log G vs log n_z are shown in Figure 4. From these plots and Table II we deduce with the help of eq 31 and 32 that y in $\beta \propto n^{-y}$ is

$$y = 1.0 \pm 0.2 \tag{38}$$

which clearly supports the simple steady-state reptation model. This result is not changed significantly if differences of 1 or 2 °C above and below $\bar{\Delta}T_{I\to II}$ = 16.46 °C rather than 1.5 °C are used in the treatment.

The rather large standard deviations of s in both regimes I and II can be traced in large part to the variation from one fraction to another of $\Delta T_{I\to II}$. The seemingly small variation of ±0.39 °C about the mean of 16.46 °C evident in Table I is enough to explain most of the deviation in s. The uncertainty in y is a combination of the standard deviation in s and the uncertainty in λ. We consider it highly probable that the true value of the exponent y is within the bounds ±0.2 of unity. Despite the extensive data base, it was not possible to distinguish the predicted $G_I \propto n^{-4/3}$ law for regime I from the $G_{II} \propto n^{-7/6}$ law predicted for regime II.

An analysis using $n_w = M_w/14.03$ instead of n_z to construct plots of log G vs log n_w analogous to those in Figure 4 led to somewhat larger s values and a substantially larger standard deviation for regime I. The latter provides an argument from an experimental point of view for a function closer to n_z than n_w being the controlling parameter in the steady-state reptation process. (There is no reason to consider the corresponding number average plots). It is evident from this and other considerations mentioned earlier that the reptation rate is governed more by the longer molecules in the system, as is represented to a sufficient approximation in the plots of log G vs log n_z.

A way of summarizing the kinetic results is to combine what is known from both theory and experiment in the growth rate expressions (eq 26a and 27a) for regime I and II in numerical form as

$$G_I \text{ (cm s}^{-1}) = \left(\frac{2.841 \times 10^{13}}{n_z^{4/3}}\right)(\Delta T)e^{-5736/RT}e^{-1.91\times10^5/T(\Delta T)} \tag{39}$$

$$G_{II} \text{ (cm s}^{-1}) = \left(\frac{2.836 \times 10^{6}}{n_z^{7/6}}\right)(\Delta T)e^{-5736/RT}e^{-0.955\times10^5/T(\Delta T)} \tag{40}$$

where $\Delta T = T_m - T$ is to be calculated for each fraction by using the T_m from eq 35. Here 2.841×10^{13} is recognized as $Z_{I(\lambda)}$ and 2.836×10^6 as $Z_{II(\lambda)}$, both in the units cm s^{-1} deg^{-1}. The quantity $Z_{I(\lambda)}/Z_{II(\lambda)}^2$ is 3.53_2 deg s cm^{-1}, which value was earlier useful in estimating n_L and thence the substrate length L with eq 33.

Equations 39 and 40 provide a good fit to the experimental growth rate data. They reproduce the data for G_I and G_{II} given in Table I at ΔT = 14.96 °C for regime I and ΔT = 17.96 °C for regime II within 40% and 41%, respectively. (These figures represent standard deviations.) The fit with eq 39 and 40 is noticeably better than can be obtained if each preexponential is taken to vary as n^{-1} rather than as $n^{-4/3}$ and $n^{-7/6}$. We note however that if the preexponential factors for G_I and G_{II} are both allowed to vary as n^{-1} as in a previous exposition,[2] the fit is still far better than if the preexponentials are assumed to be invariant with n.

Table II
Experimental Values of s and Estimates of y from Polyethylene Fractions Crystallized from the Melt

regime	exptl values of s in $G_{\Delta T\text{const}} \propto n^{-s}$[d]	estimates[a] of y in $\beta \propto n^{-y}$		
		λ = $^1/_3$ (ϕ = 270°)	λ = 0.408 (ϕ = 220.5°)[e]	λ = $^1/_2$ (ϕ = 180°)
regime I ΔT = 14.96 °C	$s_I = 1.32 \pm 0.20$ (cc = 0.894)	0.99 ± 0.20[b]	0.91 ± 0.20[b]	0.82 ± 0.20[b]
regime II ΔT = 17.96 °C	$s_{II} = 1.35 \pm 0.20$ (cc = 0.902)	1.18 ± 0.20[c]	1.15 ± 0.20[c]	1.10 ± 0.20[c]
		$\langle y \rangle = 1.08_5 \pm 0.18$	$\langle y \rangle = 1.03 \pm 0.19$	$\langle y \rangle = 0.96 \pm 0.20$

[a] The value $y = 1.0 \pm 0.2$ covers all the entries in the table, including those pertinent to the upper and lower bonds of λ. This is employed in the text as the reported value. (The grand average of all values listed is $\langle y \rangle = 1.02_5 \pm 0.15_3$). The errors correspond to standard deviations, and "cc" is the correlation coefficient. In the case of the estimates of $\langle y \rangle$ for each choice of λ above, the standard deviations include the difference in s that occurs between regime I and regime II. [b] y calculated from eq 31. [c] y calculated from eq 32. [d] Eleven fractions n_z = 1590 to n_z = 14 500. [e] log mean of λ = $^1/_3$ and $^1/_2$.

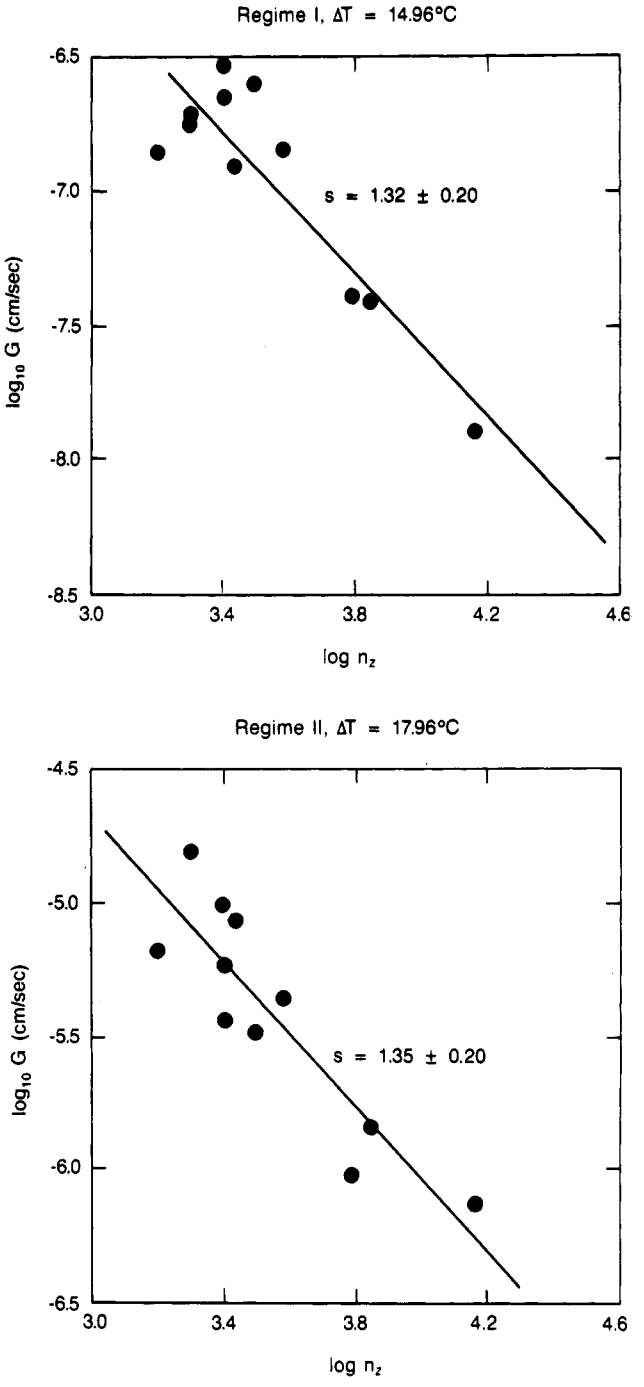

Figure 4. Plots of log $G_{\Delta T\text{const}}$ vs log n_z for the 11 polyethylene fractions n_z = 1590 to n_z = 14 500 employed to determine s_I and s_{II}. The results imply that y is 1.0 ± 0.20 (see Table II), which supports the steady-state reptation model.

Because the power of n is different for G_I and G_{II} in eq 39 and 40, the undercooling where the regime I → II transition occurs, i.e., where $G_I = G_{II}$, is predicted to shift slightly with changing n_z. The calculated value of $\overline{\Delta T}_{I\to II}$ depends sensitively on the ratio $Z_{I(\lambda)}/Z_{II(\lambda)}$. The $\Delta T_{I\to II}$ predicted from eq 39 and 40 by setting $G_I = G_{II}$ is 16.06 °C for n = 1590 and 16.39 °C for n = 14 500. The average undercooling predicted with eq 39 and 40 at the regime I → II transition is thus $\overline{\Delta T}_{I\to II}$ = 16.22 ± 0.17 °C, which is to be compared to the experimental value $\overline{\Delta T}_{I\to II}$ = 16.46 ± 0.39 °C exhibited in Table I. It may be concluded that eq 39 and 40 provide an accurate and meaningful representation of the growth rate data inasmuch as they reproduce the absolute growth rates in both regimes I and II as a function of molecular weight and temperature within experimental error and at the same time yield the correct mean undercooling at the regime I → II transition. The analysis is further supported by the fact that the ratio $Z_{I(\lambda)}/Z_{II(\lambda)}^2$ leads with eq 33 or eq A-15 to a sensible value of L that is consistent with the failure to observe nonlineal growth in very small crystals even with a sophisticated measurement technique.[36]

IV. Discussion and Conclusions

Consider first the implications of the present study concerning reptation as a transport process in the melt of a high molecular weight polymer. It is clearly evident from our result $y \cong 1$ that the chain being drawn onto the crystal by the force of crystallization exerts a resistance to this force that is essentially proportional to its length. Further, the overall time is remarkably short which is caused by the combination of a normal friction coefficient of $\sim 10^{-9}$ erg s cm^{-2} and a strong "reeling in" force. (A simple calculation with either eq 9 or 10 shows that at $\overline{\Delta T}$ = 16.46 °C the mean force $\bar{f}_c$ is $\sim 7 \times 10^{-9}$ dynes; this force is drawing on a chain of cross-sectional area $a_0 b_0 = 18.88 \times 10^{-16}$ cm^2 and corresponds to a pressure equivalent to 3.7 atm urging the chain from the tube onto the growth front.) Under these circumstances, the concept of steady-state curvilinear motion in a reptation tube appears highly plausible. There is little time available for lateral motion of the tube or major excursions from it. The chain end is drawn toward the crystal and the tube simply disappears. Neither is the mean force $\bar{f}_c$ in the vicinity of the regime I → II transition so great that the molecule cannot respond over its entire remaining length in the available time as the result $y \cong 1$ conclusively shows. Elsewhere we have shown with an earlier version[2] of the present type of treatment that at large undercoolings, where $\bar{f}_c$ is large and the nucleation rate i extremely high as at the onset of regime III, only relatively short sections of chain involving "slack" in the tube can be transported to the growth front. This was anticipated by Klein and Ball.[6] As treated by Klein and Ball, pure reptation of slack does not depend on molecular weight; i.e., one has $y \sim 0$.

The present result $y \cong 1$ implying the validity of the steady-state reptation model in polyethylene in regimes I and II would almost certainly not apply if "solvent" molecules consisting of uncrystallizable rejected species of low molecular weight were present, which would greatly facilitate lateral motion of the tube. In such a case one would expect as a rough approximation that G_{II} would be proportional to $n^{-(0.5+\lambda/2)}$ or $\sim n^{-2/3}$; i.e., $s_{II} \simeq {}^2/_3$. From the careful study by Vasanthakumari and Pennings[27] on four fractions of poly(L-lactic acid) we estimate that $s \cong 0.53$ in regime II. There is no evidence that the low molecular weight components were removed in this case. We have also estimated values of s from other studies in the literature as follows: poly(3,3-diethyloxetane),[39] $s \cong 0.5$; poly(hexamethylene sulfide),[40] $s \cong 0.7$; and i-poly(1-butene),[41] $s \cong 0.6$. Again, there is no evidence that the low molecular weight components were removed.

The results obtained here have significance related to the application of nucleation theory to crystallization with chain folding. Of foremost importance is that part of the theory dealing with the reptation process which, taking place under the influence of a relatively strong force, allows molecules readily to be drawn from the interentangled melt onto the growth front with sufficient rapidity to allow considerable regular folding. It is evident that this is true in regimes I and II in polyethylene in the molecular weight range treated here, notwithstanding arguments to the contrary.[18] Even in regime III, the slack is sufficient to allow small chain-folded clusters with two or three stems

to form.[2,6] The chain-folded clusters will of course vary in size. This leads to the so-called "variable cluster" model[30,42] of chain folding in crystallization from the melt. In any event, the gambler's ruin limit requires clusters of at least this size in order to avoid a density paradox at the lamellar surface.[42-45] Larger clusters can form in regimes I and II, where steady-state reptation can occur.

The present demonstration that $y \cong 1$ does not imply that each long molecule is drawn onto the growth front in a perfect chain-folded sequence. A given molecule is drawn for a time onto the growth front at a rate dependent on its remaining length, thus forming a chain-folded cluster. Then an interuption by "strange" molecule may take place. The pendant chain of the original molecule will shortly find a niche and resume the substrate completion process, the remainder of the chain being drawn as before through a reptation tube. The interruptions lead to some nonadjacent reentry and the concomitant amorphous component.

We note that the treatment given here will become inapplicable when the molecules are so long that most of them nucleate on two or more different lamellae or at distant points on the same lamella. Such molecules are thereby prevented from "complete" crystallization and cannot exhibit $y \cong 1$, i.e., steady-state reptation behavior. This clearly does not happen in polyethylene to a degree sufficient to prevent a determination of y up to molecular weights of ca. $n_z = 14\,500$ ($M_z \cong 200\,000$). At this and lower molecular weights some interlamellar links are undoubtedly present—the gambler's ruin calculation[43,44] indicates that perhaps one in ten to twenty of the surface sites where chains emerge are involved in such links. The same calculation suggests that an even larger fraction of the surface sites involve chains that reenter the same lamella at a distant point. Some of these chains ("loose loops") are intertwined with those of the adjacent lamella, forming another kind of interlamellar "link".[46] All this allows a certain amount of the toughness of polyethylene in this molecular weight range to be attributed to interlamellar links. Nevertheless a significant fraction of the chains—probably in the vicinity of two-thirds—participate in the steady-state reptation process. Thus in the range near and below $M_z \cong 200\,000$ we were able readily to detect the effect of steady-state reptation and determine its behavior. The expected failure to have enough molecules unencumbered by multiple nucleation to engage in simple steady-state reptation began somewhat above $M_z \cong 200\,000$, where the diffuseness of the regime I → II transition prevented an analysis. This coincides rather closely with the point where the ultimate degree of crystallinity begins to drop markedly with a further increase in molecular weight.[47,48] This drop is a clear sign that most of the molecules were now so long that they repeatedly engaged in multiple nucleation either within the same lamella or between one or more lamellae, thus accounting for the increased fraction of amorphous phase. Then much of the crystallization, though in the chain-folded "variable cluster" model[30,42] mode, occurs by reptation of slack rather than steady-state reptation.

The above-mentioned decrease in degree of crystallinity with increasing molecular weight can be rationalized in terms of the root-mean-square radius of gyration r_g as it relates to the lamellar thickness l_g^*. As noted earlier, l_g^* for polyethylene is ca. 169 Å at the regime I → II transition. From the well-known formula

$$r_g = \langle S^2 \rangle^{1/2} = (C_n/6)^{1/2}(n l_u^2)^{1/2} \qquad (41)$$

one finds (with $C_n = 6.7$) that $r_g = 53.5$ Å for $n = 1590$ and $r_g = 162$ Å for $n = 14\,500$. Thus, it would appear that when the radius of gyration becomes somewhat larger than the lamellar thickness, excursions of once pinned molecules to different nearby lamellae forming irresolvable amorphous ties between them can become more frequent and thereby markedly reduce the degree of crystallinity. Of course there are some such excursions even when the radius of gyration is less than l_g^*. The above calculation is approximate because the effective r_g is affected by the presence of the crystal. Nevertheless, we expect that the overall concept is tenable. A corollary of the above is that the upper bound of the thickness of the amorphous zone between the chain-folded lamellae, l_a, should correspond approximately to r_g. That degree of crystallinity measurements on polyethylene fractions indicate that l_a corresponds rather closely to r_g will be dealt with in another publication.

The revised treatments of regime I and regime II presented here lead to eq 26 and 27, and the corresponding data analysis leads to eq 39 and 40. These are quite similar in form to those in common use, except that the molecular weight and ΔT dependence of the preexponential factors are more detailed; the makeup of both $K_{g(I)}$ and $K_{g(II)}$ and the role of Q_D^* is identical with that of previous treatments. Some expressions in common use are of the form[14] $G = G_0 \exp(-Q_D^*/RT) \exp[-K_g/T(\Delta T)]$ and $G = (C/n) \exp(-Q_D^*/RT) \exp[-K_g/T(\Delta T)]$. For a given set of input data, plots of $\ln G + Q_D^*/RT - \ln(\Delta T)$ vs $1/T(\Delta T)$ and $\ln G + Q_D^*/RT$ vs $1/T(\Delta T)$ lead to virtually identical K_g values, but the most meaningful preexponential factors ($Z_{I(\lambda)}$ and $Z_{II(\lambda)}$) are obtained from the first type of plot mentioned. For applications that include data at low crystallization temperatures, $\exp(-Q_D^*/RT)$ must be replaced by a function of the form[49,50] $\exp[-U^*/R(T - T_\infty)]$. Perhaps this is to be interpreted as meaning that all motion in the new shrunken reptation tube, including that of slack, is forbidden below T_∞.

From the standpoint of making an estimate of the substrate ("persistence") length L from the experimental values of the preexponential factors, i.e., from $Z_{I(\lambda)}$ and $Z_{II(\lambda)}$, the present treatment is distinctly superior to earlier ones. The new value of $L \simeq 210$ Å, which we take to be correct within a factor of about 2 and which is relevant to the 110 face, is such that one cannot expect to observe growth that is nonlineal in time: it would be extremely difficult to measure the growth rate of crystals of this size. As noted earlier, this removes an objection to nucleation theory that had been raised by Point et al.[36] The above result for L holds irrespective of whether or not the backward reaction (stem removal) is considered. Considering its small size and general nature, we doubt that L corresponds to any obvious physical feature on the crystal edge as examined, say, by electron microscopy, nor to the full edge of any crystal of normal dimensions. In fact, the lower bound of L, which we judge to be ca. 100 Å, is even small enough to allow a slight amount of macroscopic curvature on the 110 face of a crystal exhibiting regime I behavior.

Though the existence of the substrate length L is assured by the well-documented appearance in the various polymers mentioned previously of the regime I → II transition, its precise physical origin is still the subject of speculation. Clearly some agency in effect breaks up the growth front into apparently independent sections of mean length L. It would appear that L represents the mean distance ("persistence length") between "stopping" defects of some type that occur on the substrate, in which situation the puzzle becomes that of elucidating the nature of the defect. We note in this connection that X-ray linewidth measurements on polymer crystals, including polyethylene,[51,52]

commonly suggest a loss of stem correlation over distances of roughly 100–500 Å, the lower figure being in the range we have estimated for L by the kinetic method. The precise physical origin of this stem correlation length is not known though one could suppose it might well have to do with strain resulting from repulsion of chain folds. One cannot disregard the possibility that L and the X-ray stem correlation length have a common origin. Frank[24] originally suggested that L might correspond to the boundaries of imperfect lattice coherence.

The treatment in the body of the paper with $\epsilon = 0$ (no backward reaction, B and $B_1 = 0$) and with $\epsilon = 1$ (full backward reaction with B and B_1 as represented in the Appendix) gives equations for G_I and G_{II} identical in form to eq 26 and 27 or eq 39 and 40. In particular, the dependence of these growth rates on molecular weight and undercooling is exactly the same for $\epsilon = 1$ and $\epsilon = 0$. Thus the analysis leading to the conclusion $y \cong 1$ is broadly valid. Furthermore, with identical input data for ζ_0, σ, σ_e, etc, the substrate completion rate g and the substrate length L are the same irrespective of whether $\epsilon = 0$ or $\epsilon = 1$. Only the absolute nucleation rate i and the parameter δ are different, but only by a factor of 2, which is trivial.

It is of interest to indicate further our reasons for detailing the $\epsilon = 0$ case and employing it in parallel with the $\epsilon = 1$ case to show the similarity. The $\epsilon = 0$ case is somewhat simpler and, in our view, more nearly correct in terms of the physics involved at the relatively large undercoolings considered here. We do not expect significant stem removal at such undercoolings; detailed balance, corresponding to $\epsilon = 1$, must indeed occur just at the melting point but need not apply at moderate and large undercoolings. (Recall again that regimes I, II, and III have been modeled in some detail by considering the forward reactions only.[21]) Another reason for including the $\epsilon = 0$ case is that, like the $\epsilon = 1$ case, it is amenable to the introduction of lattice strain effects that reduce the substrate completion rate to the point where a crystal edge is curved. Decidedly curved edges occur under special experimental conditions on the lateral 200-type face of polyethylene crystals, though the corresponding 110 face in the same crystal is straight or nearly so.[26,53] These curved edges have in one instance[54] been thought to represent a seemingly irreducible contradiction to nucleation theory. By solving exactly the relevant differential equations, which involve moving boundary conditions, Mansfield[55] has shown that a curved growth front will arise if the substrate completion rate g thereon becomes comparable to the rate of advance h of the edge of the crystal perpendicular to the direction of growth under consideration. The curved edge is a section of an ellipse. Only a small amount of lattice strain is required to reduce the value of g in the affected sector to the point that marked curvature is predicted. In a general framework, curved edges can be predicted even in the absence of lattice strain, but the introduction of a small degree of lattice strain accentuates the effect and can even reverse the behavior with temperature. Thus it would appear that nucleation theory, as emended if necessary to accommodate lattice strain in special situations, is capable of dealing in a direct way with the problem of curved edges. Details will be presented elsewhere.[56]

We close with the observation that the form of nucleation theory espoused here, whose early origins are to be found in conceptions dealing only with atoms or small nonchain molecules, has been adapted in important ways to account for the chain character of polymer molecules. The concept of the chain fold, meaningless in the case of small atoms or molecules, has of course been included in nucleation theory for lamellar polymers from the outset.[57] The advent of "quantized" chain folding in shorter chain systems, wherein once, twice, and three times folding, etc., occurs with increasing undercooling has been quantitatively explained in terms of nucleation theory by appropriately modifying the mean fold surface free energy to account for the chain ends.[58] In the present work we have for a high polymer accounted for the free energy change associated with the first attachment of a chain and shown its effect on the molecular weight dependence of the growth rate. Also we have here and elsewhere[2] introduced the concept of the configurational path degeneracy, arising in part from the chain character of the numerous molecules attached to the substrate prior to the time that one eventually forms an aligned stem. This concept leads to an understanding of the large numerical value of C_0 and thence the large numerical values of the preexponential factors $Z_{I(\lambda)}$ and $Z_{II(\lambda)}$ that are observed experimentally. While not yet fully detailed, the present work nevertheless provides insights, based on the chain character of the molecules, concerning the origin and thickness of the amorphous zone. In addition, one knows that the gambler's ruin laws, derived from the properties of chains emerging from a plane surface, place an absolute lower bound on the degree of adjacent or very near adjacent reentry in lamellar systems.[43-45] Though the subject will be dealt with in more detail elsewhere, we mention that the problem of the failure of long molecules to nucleate in the apparently favorable site at the apex of a large V-shaped notch, where ϕ is significantly less than 180°, has been addressed.[59] One part of this argument is based on calculations showing that a normal density of chain segments can build up at the notch site for short molecules but only a much lower density for a very long molecules. Here again one sees the effect of chain character on polymer nucleation. Perhaps most important of all from a broad perspective, reptation theory, with its clearly evident dependence on chain character, has herein been brought into the nucleation theory for polymer crystallization with chain folding in such a way as to facilitate a test of an important aspect of the reptation concept itself. Thus, we have shown that under definitely specifiable conditions, the simple steady-state reptation model is tenable for a high molecular weight polymer melt.[60]

Appendix. Formulas for Case "$\epsilon = 1$" Where Backward Reaction Is Fully Active

Begin with the rate constants for the forward and backward reactions of stem addition

$$A_0 = {}^1\beta(x_0/l_0)^\lambda e^{-2b_0\sigma l/kT} \tag{A-1}$$

$$B_1 = {}^1\beta e^{-a_0b_0l(\Delta G)/kT} \tag{A-2}$$

$$A = {}^1\beta e^{-q/kT} \tag{A-3}$$

$$B = {}^1\beta e^{-a_0b_0l(\Delta G)/kT} = B_1 \tag{A-4}$$

as noted in Figure 2. In this situation A_0/B_1 and A/B recover the equilibrium distribution consistent with eq 2, so that detailed balance holds. Then one has

$$g_{nuc} \equiv a_0(A - B) = a_0{}^1\beta e^{-q/kT}[1 - e^{-a_0b_0\delta(\Delta G)/kT}] \tag{A-5}$$

$$g_{nuc} \cong a_0{}^1\beta[a_0(\Delta G)/\sigma]e^{-q/kT}$$

where we have used $\delta \cong kT/b_0\sigma$ from the last term in[14,25]

$$l = \langle l \rangle = l_g^* = 2\sigma_e/\Delta G + \frac{kT}{2b_0\sigma}\left[\frac{(4\sigma/a_0) + \Delta G}{(2\sigma/a_0) + \Delta G}\right] \tag{A-6}$$

Setting eq A-5 equal to g_{rept} of the text (eq 13), one gets

$$ {}^1\beta = (1/n)\left[\frac{b_0\sigma \exp(Q_D^*/RT_0)}{\zeta_0 l_f}\right]e^{-Q_D^*/RT} \quad \text{(A-7)} $$

Redefining the retardation parameter as

$$ {}^1\beta = \left(\frac{{}^1\kappa}{n}\right)\left(\frac{kT}{h}\right)e^{-Q_D^*/RT} \quad \text{(A-8)} $$

one gets

$$ {}^1\kappa = \left(\frac{h}{kT}\right)\frac{b_0\sigma \exp(Q_D^*/RT_0)}{\zeta_0 l_f} \quad \text{(A-9)} $$

which is 0.330 for the input data given in the text (Q_D^* = 5736 cal mol^{-1}, T_0 = 450 K, $b_0 = 4.15 \times 10^{-8}$ cm, σ = 11.8 erg cm^{-2}, T = 401.7 K, $\zeta_0 = 10^{-9}$ erg s cm^{-2}, $l_f = 10.86 \times 10^{-8}$ cm). Upper left-hand superscripts on β, κ, and Z denote the value of ϵ.

The nucleation rate is

$$ i = S_T/n_L a_0 = \left(\frac{1}{n_L a_0}\right)\left(\frac{1}{l_u}\right)\int_{2\sigma_e/(\Delta G)}^{\infty}\frac{N_0 A_0(A-B)}{A-B+B_1}\,dl \quad \text{(A-10)} $$

$$ i \cong C_0{}^1\beta(x_0/l_u)^\lambda(1/n^\lambda)(1/a_0)\left(\frac{kT}{2b_0\sigma l_u}\right)\times \left(\frac{a_0(\Delta h_f)}{2\sigma}\right)\frac{\Delta T}{T_m}e^{-4b_0\sigma\sigma_e/\Delta GkT} $$

This leads to the growth rate in regime I for the case ϵ = 1 (identical in form with eq 26a)

$$ G_I \equiv b_0 i n_L a_0 = \frac{{}^1Z_{I(\lambda)}}{n^{1+\lambda}}\Delta T e^{-Q_D^*/RT}e^{-K_{g(I)}/T(\Delta T)} \quad \text{(A-11)} $$

where $K_{g(I)}$ is the same as given in eq 26c but with

$$ {}^1Z_{I(\lambda)} = C_0{}^1\kappa n_L\left(\frac{b_0kT}{h}\right)\left(\frac{x_0}{l_u}\right)^\lambda\left(\frac{1}{T_m}\right)\left(\frac{kT}{2b_0\sigma l_u}\right)\times \left(\frac{a_0(\Delta h_f)}{2\sigma}\right) = Z_{I(\lambda)}/2 \quad \text{(A-12)} $$

which is to be compared with eq 26b. For regime II

$$ G_{II} \equiv b_0(2ig)^{1/2} = \frac{{}^1Z_{II(\lambda)}}{n^{1+\lambda/2}}\Delta T e^{-Q_D^*/RT}e^{-K_{g(II)}/T(\Delta T)} \quad \text{(A-13)} $$

which is identical in form with eq 27a, and where $K_{g(II)}$ is identical with eq 27c. However, the preexponential differs from the "ϵ = 0" case according to

$$ {}^1Z_{II(\lambda)} = C_0{}^{1/2}\,{}^1\kappa(x_0/l_u)^{\lambda/2}\left(\frac{b_0kT}{h}\right)\left(\frac{a_0(\Delta h_f)}{\sigma}\right)\times \left(\frac{kT}{2b_0\sigma l_u}\right)^{1/2}\left(\frac{1}{T_m}\right)e^{-q/2kT} = Z_{II(\lambda)}/\sqrt{2} \quad \text{(A-14)} $$

From (A-12) and (A-14) one gets

$$ n_L = 2{}^1\kappa\left(\frac{b_0kT}{h}\right)\left(\frac{1}{T_m}\right)\left[\frac{a_0(\Delta h_f)}{\sigma}\right]\left[\frac{{}^1Z_{I(\lambda)}}{{}^1Z_{II(\lambda)}{}^2}\right]e^{-q/kT} \quad \text{(A-15)} $$

For a given value of ζ_0 and l_f, the factor ${}^1\kappa[a_0(\Delta h_f)/\sigma]$ is numerically identical with the κ of eq 17b, so for a specified set of input data the substrate length L is unchanged by the assumption that the backward reactions (A-2) and (A-4) are fully active. The absolute value of g is also unchanged. The main effect of the inclusion of the backward reactions is to slow down the nucleation rate i by a factor of 2 and to increase δ by the same factor. The overall conclusion is then that there are no differences in the temperature and molecular weight dependences of G_I, G_{II}, the substrate completion rate g, or the substrate length L, in the "ϵ = 0" and "ϵ = 1" cases. The role of reptation in the melt is physically identical for ϵ = 1 and ϵ = 0.

Acknowledgment. The authors wish to thank Professor Dale S. Pearson, University of California, Santa Barbara, for a private communication concerning the monomeric friction coefficient of polyethylene. Thanks are also due Drs. E. A. DiMarzio and C. M. Guttman of the National Bureau of Standards and Dr. M. L. Mansfield of MMI for their helpful comments. This work was partially supported (J.D.H.) by Grant DMR 86-07707, Polymers Program, Division of Materials Research, of the National Science Foundation.

Registry No. Polyethylene, 9002-88-4.

References and Notes

(1) de Gennes, P.-G. *J. Chem. Phys.* **1971**, *55*, 672.
(2) Hoffman, J. D. *Polymer* **1982**, *23*, 656.
(3) Hoffman, J. D.; Guttman, C. M.; DiMarzio, E. A. *Faraday Discuss. Chem. Soc.* **1979**, *No. 68*, 177.
(4) Hoffman, J. D.; Frolen, L. J.; Ross, G. S.; Lauritzen, J. I., Jr. *J. Res. Natl. Bur. Stand., Sect. A* **1975**, *79*, 671.
(5) DiMarzio, E. A.; Guttman, C. M.; Hoffman, J. D. *Faraday Discuss. Chem. Soc.* **1979**, *No. 68*, 210.
(6) Klein, J.; Ball, R. *Faraday Discuss. Chem. Soc.* **1979**, *No. 68*, 198.
(7) Keith, H. D.; Padden, F. J., Jr. *J. Appl. Phys.* **1963**, *34*, 2409.
(8) Keith, H. D.; Padden, F. J., Jr. *J. Appl. Phys.* **1964**, *35*, 1270.
(9) Keith, H. D.; Padden, F. J., Jr. *J. Appl. Phys.* **1964**, *35*, 1286.
(10) DeGennes, P. G. *Macromolecules* **1976**, *9*, 587, 594.
(11) de Gennes, P.-G.; Legêr, L. *Annu. Rev. Phys. Chem.* **1982**, *33*, 49.
(12) Doi, M.; *J. Polym. Sci., Polym. Lett. Ed.* **1981**, *19*, 265.
(13) Doi, M.; Edwards, S. F. *The Theory of Polymer Chain Dynamics*; Clarendon: Oxford, 1986; Chapter 7.
(14) Hoffman, J. D.; Davis, G. T.; Lauritzen, J. I., Jr. In *Treatise on Solid State Chemistry*; Hannay, N. B., Ed.; Plenum: New York, 1976; Vol. 3, Chapter 7, pp 497–614.
(15) Lauritzen, J. I., Jr.; DiMarzio, E. A. *J. Res. Natl. Bur. Stand. (U.S.)* **1978**, *83*, 381.
(16) Fletcher, D. P.; Klein, J. *Polym. Commun.* **1985**, *26*, 2.
(17) Pearson gives $\zeta = 3.7 \times 10^{-11}\exp[1130/(T+100)]$ where T is in °C. Pearson, D. S., University of California, Santa Barbara, personal communication.
(18) Flory, P. J.; Yoon, D. Y. *Faraday Discuss. Chem. Soc.* **1979**, *No. 68*, 389.
(19) Berry, G. C.; Fox, T. G. *Adv. Polym. Sci.* **1967**, *5*, 261.
(20) Hoffman, J. D.; Guttman, C. M.; DiMarzio, E. A. *Faraday Discuss. Chem. Soc.* **1979**, *No. 68*, 394.
(21) Guttman, C. M.; DiMarzio, E. A. *J. Appl. Phys.* **1983**, *54*, 5541.
(22) Hoffman, J. D. *Polymer* **1985**, *26*, 803.
(23) Lauritzen, J. I., Jr. *J. Appl. Phys.* **1973**, *44*, 4353.
(24) Frank, F. C. *J. Cryst. Growth* **1974**, *22*, 233.
(25) Lauritzen, J. I., Jr.; Hoffman, J. D. *J. Appl. Phys.* **1973**, *44*, 4340.
(26) Organ, S. J.; Keller, A. *J. Polym. Sci., Polym. Phys. Ed.* **1986**, *24*, 2319.
(27) Vasanthakumari, R.; Pennings, A. J. *Polymer* **1983**, *24*, 175.
(28) Phillips, P. J.; Vantansever, N. *Macromolecules* **1987**, *20*, 2138.
(29) Alamo, R.; Fatou, J. G.; Guzman, J. *Polymer* **1982**, *23*, 379.
(30) Hoffman, J. D. *Polymer* **1983**, *24*, 3. For an earlier discussion of regime III, see: Reference 3. Hoffman, J. D. *Faraday Discuss. Chem. Soc.* **1979**, *No. 68*, 378.
(31) Pelzbauer, Z.; Galeski, A. *J. Polym. Sci., Part C* **1972**, *38*, 23.
(32) Roitman, D. B.; Marand, H. L.; Hoffman, J. D. *Bull. Am. Phys. Soc.* **1988**, *33*, 248.
(33) Clark, E. J.; Hoffman, J. D. *Macromolecules* **1984**, *17*, 878.
(34) Barham, P. J.; Keller, A.; Otun, E. L.; Holmes, P. A. *J. Mater. Sci.* **1984**, *19*, 2781.
(35) Lovinger, A. J.; Davis, D. D.; Padden, F. J., Jr. *Polymer* **1985**, *26*, 1595.
(36) Point, J. J.; Colet, M. C.; Dosiere, M. *J. Polym. Sci., Polym. Phys. Ed.* **1986**, *24*, 357.

(37) Stromberg, R. R.; Grant, W. H.; Passaglia, E. *J. Res. Natl. Bur. Stand., Sect. A* **1964**, *68*, 391.
(38) Flory, P. J.; Vrij, A. *J. Am. Chem. Soc.* **1963**, *85*, 3548.
(39) Gomez, M. A.; Fatou, J. G.; Bello, A. *Eur. Polym. J.* **1986**, *22*, 661.
(40) Sanchez, A.; Marco, C.; Fatou, J. G.; Bello, A. *Makromol. Chem.* **1987**, *188*, 1205.
(41) Cortazar, M.; Guzman, G. M. *Makromol. Chem.* **1982**, *183*, 721.
(42) Guttman, C. M.; DiMarzio, E. A.; Hoffman, J. D. *Polymer* **1981**, *22*, 597.
(43) Guttman, C. M.; DiMarzio, E. A.; Hoffman, J. D. *Polymer* **1981**, *22*, 1466.
(44) Guttman, C. M.; DiMarzio, E. A. *Macromolecules* **1982**, *15*, 525.
(45) Mansfield, M. L. *Macromolecules* **1983**, *16*, 914.
(46) Lacher, R. C.; Bryant, J. L.; Howard, L. N. *J. Chem. Phys.* **1986**, *85*, 6147.
(47) Fatou, J. G.; Mandelkern, L. *J. Phys. Chem.* **1965**, *69*, 417.
(48) Maxfield, J.; Mandelkern, L. *Macromolecules* **1977**, *10*, 1141.
(49) Hoffman, J. D. *SPE Trans.* **1964**, *4*, 315.
(50) Suzuki, T.; Kovacs, A. J. *Polym. J. (Tokyo)* **1970**, *1*, 82.
(51) Buchanan, D. R.; Miller, R. L. *J. Appl. Phys.* **1966**, *37*, 4003.
(52) Balta Calleja, F. J.; Hosemann, R.; Wilke, W. *Makromol. Chem.* **1966**, *92*, 25.
(53) Khoury, F. *Faraday Discuss. Chem. Soc.* **1979**, *No. 68*, 404.
(54) Sadler, D. M. *Polymer* **1983**, *24*, 1401.
(55) Mansfield, M. L., submitted for publication in *Macromolecules*.
(56) Hoffman, J. D.; Miller, R. L.; Mansfield, M. L., submitted for publication.
(57) Lauritzen, J. I., Jr.; Hoffman, J. D. *J. Res. Natl. Bur. Stand., Sect. A* **1960**, *64*, 73.
(58) Hoffman, J. D. *Macromolecules* **1986**, *19*, 1124. Hoffman, J. D.; Miller, R. L., submitted for publication.
(59) Mansfield, M. L., submitted for publication.
(60) **Note Added in Proof.** It has recently been pointed out to us by Professors J. Skolnick and R. Yaris of Washington University, St. Louis, that the presence of a certain amount of the constraint release mechanism would cause a tendency for β to vary more nearly as $1/n_z$ rather than $1/n_w$. (The constraint release mechanism accounts for the fact that the chains forming the reptation tube of a particular molecule in a pure polymeric liquid are themselves reptating.) As noted, our data analysis suggests that the fit with $1/n_z$ as depicted in Figure 4 is somewhat better than that with $1/n_w$. Thus it would appear that while the simple steady-state reptation model with $y \simeq 1$ certainly holds with respect to its main features in the present application, there is a hint in the results that some constraint release may occur despite the rapidity with which the chains are drawn onto the crystal.

Multicomponent Forms of Polymer Solution Theories

Charles J. Glover* and William A. Ruff†

Department of Chemical Engineering, Texas A&M University, College Station, Texas 77843-3122. *Received November 12, 1987; Revised Manuscript Received February 29, 1988*

ABSTRACT: Equation-of-state polymer solution theories provide a rational means of describing polymer solution vapor/liquid equilibrium and liquid/liquid equilibrium for multicomponent systems. These theories require a relatively small number of parameters to describe solution behavior but are quite complex and cumbersome for manipulation and calculation. This work presents an efficient mathematical framework for manipulating these equations for the purpose of deriving solution thermodynamic properties such as species activities or chemical potentials. Writing the equations in matrix form and obtaining an expression for the excess free energy provide a route to species activities which is relatively clean and compact. The resulting multicomponent equation for species activities for the Flory equation of state theory, the simplified Flory theory, and the Sanchez and Lacombe lattice fluid theory can all be obtained in a similar way and have similar forms. The compact form allows easy comparison of different theories and also provides a convenient form for coding computer calculations of solution behavior.

Introduction

The theories of Flory[1] and of Huggins,[2] based upon an incompressible lattice structure, provide the basic framework for more recent equation of state theories. This Flory–Huggins theory allows for combinatorial effects and energetic interactions between molecules and has been used widely to calculate the thermodynamic properties of polymer solutions. It succeeds in providing a rough representation of solvent activities in nonpolar polymer solutions with one adjustable parameter per binary pair interaction. It has also been fairly successful at approximating liquid–liquid phase equilibria and predicting upper critical solution temperature (UCST) of binary, nonpolar polymer solutions.[3]

Equation-of-state theories such as those by Flory[4] and by Sanchez and Lacombe[5] have extended the foundation for these types of equations by beginning with a partition function which can be used to rigorously derive equations of state and other thermodynamic relations such as species activities. The Flory theory is based upon earlier work by Prigogine,[6,7] and the Sanchez–Lacombe theory is based upon a fluid lattice, that is, one which allows for holes or unoccupied cells of the lattice in addition to cells occupied by molecular segments. The theories are successful in predicting both UCST and LCST behavior. Furthermore, they are not restricted to single-polymer systems, and, in principle, may be applied to nonpolymeric liquid solutions and multiple-polymer solutions as well. In this latter context, they have been used to aid in understanding polymer compatibility in polymer blends. Additionally, the Sanchez–Lacombe equation of state is capable of describing fluids in both the liquid and vapor states.

While these theories have the advantage, in multicomponent systems, of requiring a small number of adjustable parameters, they do suffer from the difficulty of being quite complex and unwieldy. For multicomponent systems the number of terms in the equations becomes very large, and organizing and manipulating the terms to obtain expressions for the various thermodynamic relations and computing the quantities by using these relations are quite difficult and complex.

The objective of this paper is to present a matrix approach to deriving and manipulating the multicomponent solution theory equations. This approach is both simplified in method and compact in form. In addition, this paper provides a convenient and unified review, summary,

* Author to whom correspondence may be sent.
† Present address: Texaco Research, P.O. Box 1608, Port Arthur, TX 77641.

0024-9297/88/2221-3051$01.50/0